Effects of different TMAH texturing conditions towards morphology and surface reflectivity of monocrystalline silicon for solar cells applications

M. Z. PAKHURUDDIN*, K. IBRAHIM, A. ABDUL AZIZ
Nano-Optoelectronics Research and Technology Laboratory, School of Physics, Universiti Sains Malaysia, 11800 Penang, Malaysia

In this paper, the anisotropic nature of tetramethyl ammonium hydroxide (TMAH) etchant solution (without additives) has been exploited to study the effects of various surface texturing conditions towards morphology and surface reflectivity of p-type (100) monocrystalline silicon (Si) substrates for solar cells applications. 2x2 cm^2 samples were textured at 90°C in low concentrations TMAH with different weight percentages (3 wt.%, 5 wt.% and 8 wt.%) for 10, 20 and 30 minutes respectively. The morphology of the textured samples was inspected by scanning electron microscope (SEM) and atomic force microscopy (AFM). Resulting surface reflectivity was measured on optical reflectometer. It was observed that TMAH of 5 wt.% with 10 minutes surface texturing process produced the highest density of random pyramids, highest root mean square (RMS) of surface roughness with the lowest surface reflectivity of about 7% (weighted average) within 400-1000 nm region. Higher TMAH wt.% or longer processing time resulted in a smoother wafer surface hence with higher reflectance. The results of SEM, AFM and surface reflectivity were compared to the result of a reference p-type (100) monocrystalline Si substrate (untextured) respectively. The effects of different TMAH surface texturing conditions towards the morphology and surface reflectivity of monocrystalline Si substrates for solar cells applications were subsequently discussed.

(Received December 7, 2010; accepted January 26, 2011)

Keywords: Tetramethyl ammonium hydroxide, Surface texturing, Monocrystalline, Solar cells

1. Introduction

Wet chemical etching in anisotropic etchant solutions remains the most widely used technique in Si technology due its simplicity, ease of use, low-cost and no physical damage introduced to the bulk [1]. Its wide array of applications can be found in the fabrication of microelectromechanical systems (MEMS) including sensors, actuators, nanoprobes, nanowires, laser cavities [2,3], in conventional microelectronics [4] and also in photovoltaics (PV) technologies (solar cells) [5]. Random surface texturing of crystalline silicon (c-Si) wafers is a standard technique used in PV manufacturing to reduce reflection losses from the wafer surfaces and to maximise light absorption into Si solar cells [6].

Si is known to have a high surface reflectivity of around 35% in the visible wavelength region [7]. Without any surface texturing, the incoming light (photons) gets reflected off the Si surface upon the first incidence and the photons left the surface unharnessed. With the texturing process, the planar surface of (100)-oriented wafer is transformed into a surface with random pyramids of microns in dimensions [8,9], typically bounded by intersecting four (111) equivalent planes and four <110> ridges [10] due to anisotropic etching behavior of the etchant solution (i.e. selective etching by crystal planes). With high pyramids coverage, the light (photons) impinging on the textured substrates experiences multiple reflections within the bulk (as shown by Fig. 1 below) before being reflected off. This increases the optical path length of the photons and enhances the chance of the photons being absorbed for photocurrent (i.e. electron-hole pairs) generation.

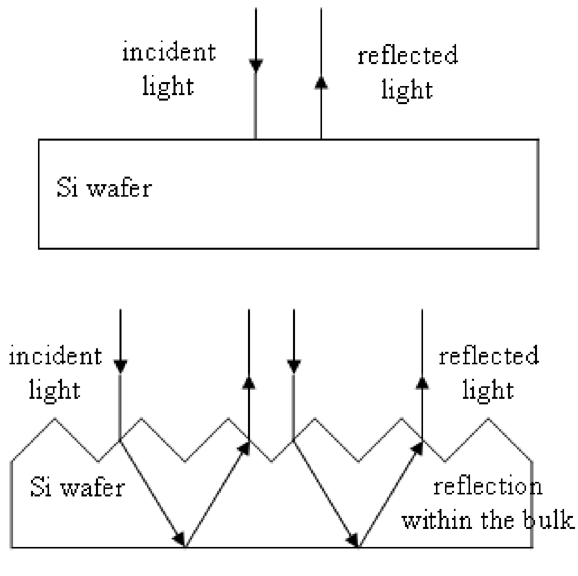

Fig. 1. Comparison of reflection mechanism on planar wafer surface (left) against textured wafer surface (right).

In commercial Si solar cells, the most widely used anisotropic etchant solution is potassium hydroxide (KOH) in water with some addition of isopropyl alcohol (IPA). However, the major drawback of KOH solution is due to its potassium contamination which is deleterious to the solar cells performance [11]. Besides, IPA has limitations due to its high cost and disposal problems apart from having low boiling point (82.5 °C) which is close to typical temperature range (70-90 °C) used in the Si solar cells texturing process. Hence, an alternative solution to KOH is a must. Tetramethyl ammonium hydroxide (TMAH) is a well-known etchant solution. It has a very high potential in Si etching since it delivers high etching rate, possesses good anisotropic properties and has been used widely in microelectronics manufacturing [12]. Most importantly, TMAH solution presents uncontaminated metal ions which is desirable for high performance solar cells [13,14].

TMAH/IPA mixture is normally used as a surface texturing agent due to the uniformity and reproducibility of the texturing results on the samples surfaces [15] but this mixture suffers from the problems related to the IPA as mentioned previously. One way to mitigate this issue is by evaluating the texturing performance of the TMAH alone (without any additives like IPA) and assess if reasonable results can be delivered.

The objective of the present work is to investigate the effects of different TMAH (without additives) texturing conditions (different concentration and texturing time) towards the morphological features and surface reflectivity of p-type (100) monocrystaline Si substrates for solar cells applications. TMAH with low range of concentrations (3-8 wt.%) coupled with short texturing times were used to perform the texturing process as these conditions are capable of producing high etching rates, extremely rough morphological features with high density of pyramids on the wafer surface [16,17] apart from being economical and practical for implementation due to low volume requirement, short processing time and simple process setup. The best process condition (i.e. process which results in the roughest surface, highest density of random pyramids with lowest surface reflectivity) will be employed in the subsequent Si solar cell fabrication to produce a device with suppressed and minimum reflection losses.

2. Experimental methods

In this experiment, p-type (100) monocrystalline Si substrates (280 μm thickness) with resistivity 1.5 Ω.cm were used to investigate the effects of different TMAH texturing conditions towards its morphology and surface reflectivity. Wafers were cut into 2x2 cm^2 samples for the texturing process. Prior to the experiment, samples were cleaned by Radio Corporation of America (RCA) technique and then dipped into 2% hydrofluoric acid (HF) solution for 5 minutes to remove native oxide. The samples were then rinsed by deionised (DI) water of high purity (18 MΩ) to remove the HF residue then dried off with nitrogen (N_2) gas. Commercial TMAH 25% was used as the etchant solution in the surface texturing process. TMAH solution was prepared in different wt.% by addition with DI water to make up a total volume (TMAH and DI water) of 40 ml per process setup. Process temperature was fixed at 90°C throughout the experiment. The samples were dipped in TMAH of different wt.% for 10, 20 and 30 minutes respectively as per Table 1 below.

Table 1. Texturing process in different TMAH wt.% under different duration (temperature fixed at 90 °C).

No.	Volume of TMAH (ml)	Volume of DI water (ml)	Calculated TMAH wt.%	Temperature (°C)	Time (min)
1	5	35	3	90	10, 20, 30
2	10	30	5	90	10, 20, 30
3	15	25	8	90	10, 20, 30

After the texturing process, morphology of the samples was inspected on scanning electron microscope (SEM) JSM 6460-LV and atomic force microscope ULTRA Objective (spot size 30×30 μm). Surface reflectivity was checked on optical reflectometer Filmetrics F20. The SEM, AFM and surface reflectivity measurement were also performed on a reference p-type (100) monocrystalline Si substrate (untextured) for comparison purpose.

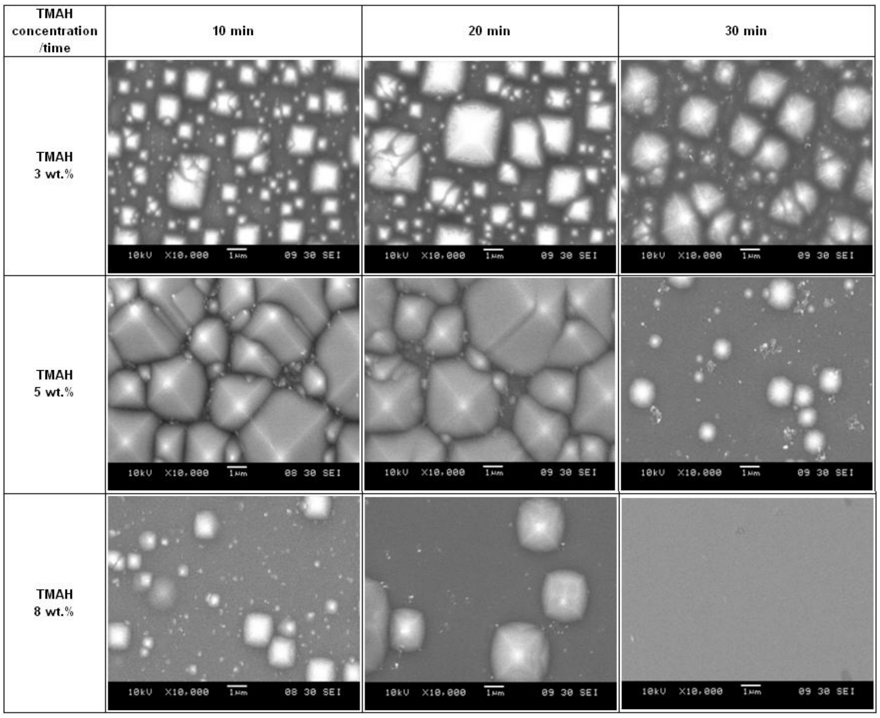

Fig. 2. Top view SEM images (10kX magnification) of samples textured at 90°C under different TMAH wt.% and process time (as of Table 1).

3. Results and discussion

Fig. 2 shows top view SEM images of p-type (100) monocrystalline Si wafers textured in TMAH of 3 wt.%, 5 wt.% and 8 wt.% under 10, 20 and 30 minutes texturing time. The SEM image of the reference sample is shown in Fig. 3 below.

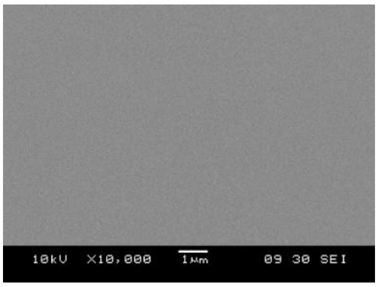

Fig. 3. Top view SEM image (10kX magnification) of p-type (100) monocrystalline wafer (untextured) as the reference sample.

In TMAH of 3 wt.%, it can be seen that the random pyramids start to form during the first 10 minutes processing time. The pyramids density is still low and they are still small in size. As the texturing time increases to 20 minutes, the pyramids density increases more significantly, covering bigger portions of the sample (around 70%). Bigger pyramids are formed. The <110> ridges start to show up. The sample appears to be physically darker in colour. After 30 minutes, pyramids cover almost 70-80% of the sample and they are more uniform in size. The (111) planes and <110> ridges can be seen more clearly. The surface of this sample becomes a bit shiny and reflective.

Increasing the volume of TMAH to 5 wt.%, it can be observed that the surface of the sample is fully covered by higher density (around 95%) of random pyramids after 10 minutes texturing time even though the pyramids size is not uniform. The (111) planes and <110> ridges can be clearly seen from the SEM picture. The sample appears dark grey in colour indicating reduced reflection losses and improved light trapping properties by the random pyramids. After 20 minutes, the pyramids are almost the same in their sizes but the sample physically looks more reflective than the previous sample (TMAH 5 wt.%, 10 minutes). After 30 minutes, the density of the pyramids reduces significantly. The sample surface is poorly covered. The random pyramids on the sample could have been over-etched at this point due to considerably long texturing time [18,19].

At TMAH of 8 wt.%, the sample appears to be very reflective as early as after 10 minutes texturing time. The wafer surface shows around 20% pyramids coverage. The density of the pyramids reduces more significantly as the texturing time increases to 20 minutes. After 30 minutes texturing process, the result shows some stains left on the surface without pyramids.

Fig. 4(a) illustrates the cross section SEM image (15kX magnification) of the sample textured in the optimum process condition (TMAH 5 wt.% for 10 minutes) as depicted by Fig. 2 earlier. This cross sectional SEM image shows packed and high density of random pyramids with their heights ranging from 0.5-6.0 μm and base widths of about the same dimensions. Fig. 4(b) is taken at an oblique angle (with 10kX magnification) to show the high density of pyramids distribution across the sample's surface. These random pyramids have the capability of trapping the incident sunlight more effectively [20], preventing it from being reflected off the surface upon the first incidence. The effective light trapping strategy causes the surface of the wafer to appear dark in colour after being textured with this process condition.

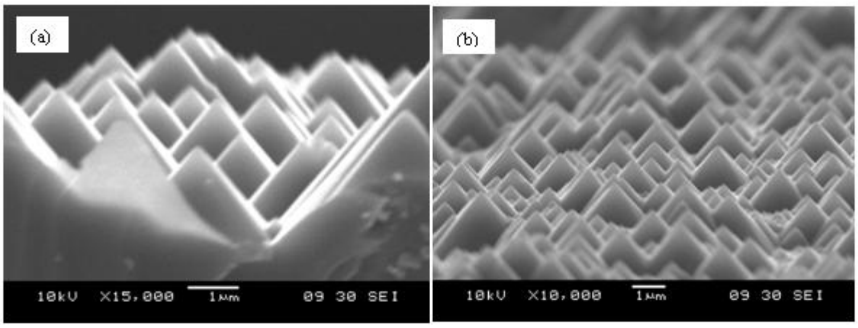

Fig. 4. (a) Cross section SEM image (15kX magnification) of the sample textured in TMAH 5 wt.% for 10 min (b) Oblique SEM image (tilted at small angle with 10kX magnification) of the same sample taken to illustrate the high pyramids density across the sample surface.

TMAH wt.% / time	10 min	20 min	30 min
TMAH 3 wt.%	RMS roughness 52.33 nm 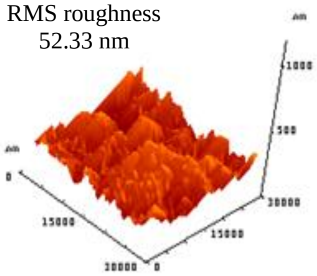	RMS roughness 82.17 nm 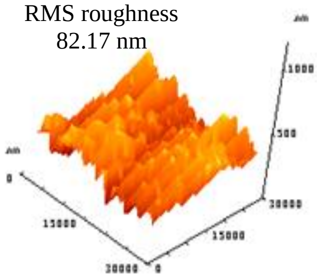	RMS roughness 97.73 nm 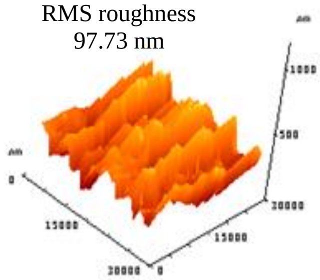
TMAH 5 wt.%	RMS roughness 224.17 nm 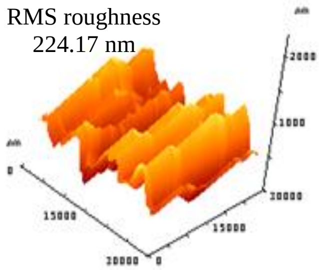	RMS roughness 187.07 nm 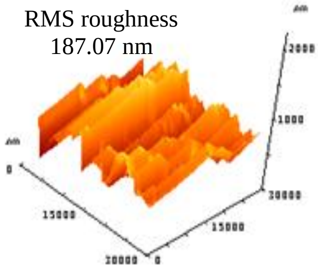	RMS roughness 54.67 nm 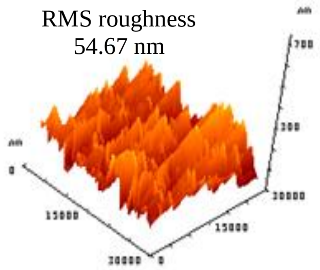
TMAH 8 wt.%	RMS roughness 52.89 nm 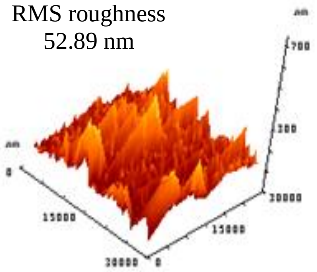	RMS roughness 36.38 nm 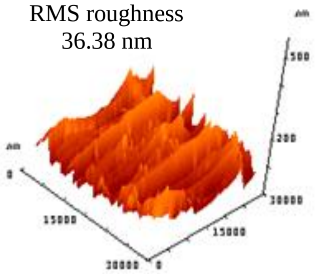	RMS roughness 14.91 nm 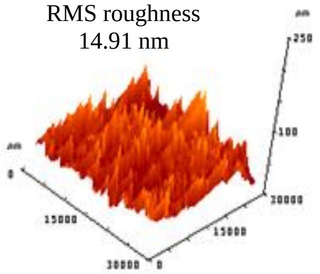

Fig. 5. AFM images of TMAH-textured samples (spot size 30×30 μm).

Fig. 5 shows the AFM images of the samples textured in all process conditions with surface roughness RMS values measured simultaneously. The AFM of the reference sample with is shown in Fig. 6 for comparison.

The reference sample possesses a very smooth surface with only 2.53 nm surface roughness RMS.

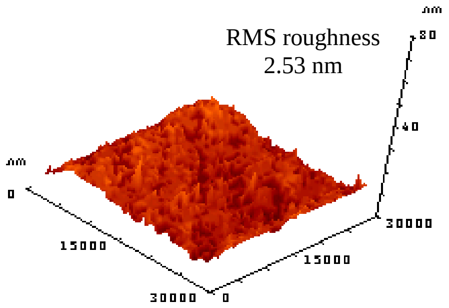

Fig. 6. AFM image of p-type (100) monocrystalline wafer as the reference sample (spot size 30x30 μm).

Fig. 7 is plotted to further explain the trend in surface roughness RMS observed in Fig. 5. From both figures (Fig. 5 and 7), it can be seen that the surface roughness increases from 52.33 nm to 97.73 nm as the texturing time increases from 10 to 30 minutes in TMAH of 3 wt.%. This data shows good corroboration with the SEM images in Fig. 2 earlier when the pyramids coverage is seen to be increasing over the texturing times, hence increasing the surface roughness.

TMAH 5 wt.% with 10 minutes reflects the optimum process setting since it produces the highest surface roughness with RMS of 224.17 nm calculated across the sample. This matches the very well with the high density of pyramids formation as observed in the SEM image previously which indirectly shows that 10 minutes is already enough to produce a highly textured surface. Under the same concentration, the RMS value reduces to 187.07 nm after 20 minutes and goes further down to 54.67 nm after 30 minutes processing.

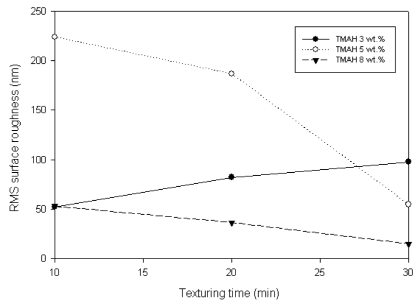

Fig. 7. Trend of RMS surface roughness under different TMAH texturing conditions (extracted from Fig. 5).

TMAH of 8 wt.% shows a very low surface roughness RMS across the texturing time, with the highest value measured as 52.89 nm after 10 minutes processing. After 30 minutes, the RMS reduces to 14.91 nm, implies a fairly smooth surface. This indicates that 8 wt.% of TMAH concentration is already too high for the application in surface texturing process.

Fig. 8-10 below are plotted to show the measurement results of surface reflectivity of all the samples with respect to the reference sample of p-type (100) monocrystalline Si substrate within the spectrum wavelength of 400-1000 nm. From these figures, it can be seen that the surface reflectivity of the reference sample is about 35%, showing how reflective the Si surface is if not treated. In the Si solar cells, the 35% of substrate reflectivity translates into high reflective losses of the incident sunlight (photons) [15]. The incident photons will be reflected off the Si surface upon the first contact and their energies cannot be harvested to create conducting electron-hole pairs in the absorber layer (Si).

Fig. 8 shows that at TMAH of 3 wt.%, the resulting values of reflectivity lie between 9-12%. The reflectivity values of the three sampling durations are quite close to each other but 20 minutes texturing process gives out the minimum value. The reflectivity data shows a good correlation with the SEM and the surface roughness AFM mentioned earlier where high density pyramids and rough surface characteristics lead to low reflectivity value. This indicates good light trapping properties exhibited by the textured samples after the treatment.

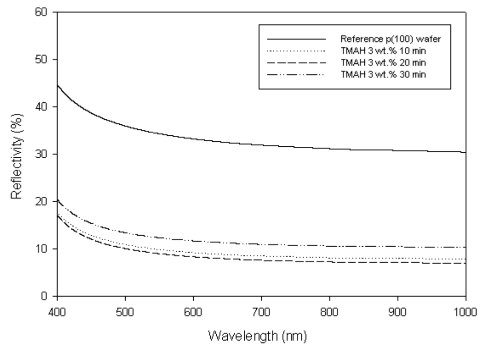

Fig. 8. Surface reflectivity of the samples textured with TMAH 3 wt.% for 10, 20 and 30 minutes.

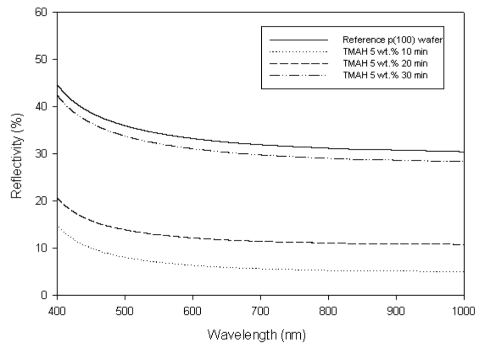

Fig. 9. Surface reflectivity of the samples textured with TMAH 5 wt.% for 10, 20 and 30 minutes.

From Fig. 9, it can be concluded that TMAH of 5 wt.% with 10 minutes texturing process produces the lowest surface reflectivity of only around 7% in average. This reserves the rest of the incoming sunlight (photons) to be absorbed or transmitted through Si (if photons energies are less than the optical band gap of Si, 1.12 eV) [21]. The value of surface reflectivity in this texturing condition substantiates the findings from the cross sectional SEM images and the calculated surface roughness RMS mentioned before and justifies why the sample appears to be dark grey in colour after the texturing process. After 20 minutes, the surface reflectivity increases to about 13% as the surface roughness RMS reduces and the value increases further, close to the reflectivity value of the reference sample after being textured for 30 minutes.

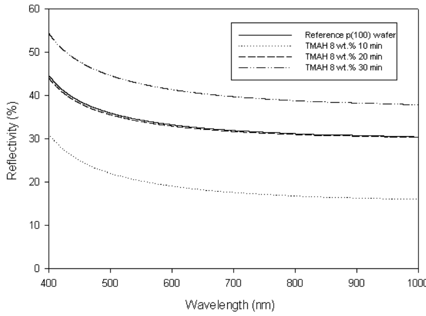

Fig. 10. Surface reflectivity of the samples textured with TMAH 8 wt.% for 10, 20 and 30 minutes.

TMAH of 8 wt.% at 10 minutes records approximately 18% surface reflectivity while the pyramids coverage is only about 20-30% on the wafer surface (as shown in Fig. 2 earlier). However, a big jump to around 35% in the reflectivity is observed as the sample texturing time reaches 20 minutes. More than 20 minutes, the reflectivity of the sample exceeds the reflectivity value of the reference wafer.

Overall, this investigation has shown that only low volume of TMAH and short duration are required to produce a highly textured (i.e. highly absorbing) Si surface as proven by the sample results in 5 wt.% of TMAH solution under 10 minutes processing, implies an economical and practical way to achieve the mentioned objective. Compatibility of TMAH to the existing microelectronics manufacturing makes it a more appealing alternative that can successfully take up the texturing process in the Si solar cells manufacturing lines.

4. Conclusions

The effects of different TMAH (without additives) texturing conditions towards morphology and surface reflectivity of p-type (100) monocrystalline Si substrates for solar cells applications have been investigated. TMAH of 5 wt.% at 10 minutes texturing time (temperature 90°C) has produced the highest density of random pyramids on the wafer surface with highest surface roughness RMS and lowest surface reflectivity within 400-1000 nm region. Higher TMAH wt.% or longer processing time resulted in a smoother wafer surface hence with higher reflectance. This investigation has highlighted the low TMAH volume along with short time requirements in order to produce a highly textured and absorbing Si hence economical and practical for implementation. High compatibility of the TMAH solution to the present microelectronics manufacturing makes it to appear more appealing to the Si PV industry.

Acknowledgement

The support of Universiti Sains Malaysia and financial assistance from Incentive Grant 1001/PFIZIK/821061 is gratefully acknowledged.

References

[1] P. Papet, O. Nichiporuk, A. Kaminski, Y. Rozier, J. Kraiem, J. F. Lelievre, A. Chaumartin, A. Fave M. Lemiti, Solar Energy Materials & Solar Cells **90**, 2319 (2006).
[2] L. Qiu, S. Hein, E. Obermeier, A. Schubert, Sensors and Actuators A **54**, 547 (1996).
[3] J. Garra, S. Brida, L. Ferrario, M. Paranjape, Sensors and Materials **13**, 351 (2001).
[4] C. S. Tan, R. Reif, Electrochemical and Solid-State Letters **8**, (12) G362 (2005).
[5] E. Manea, E. Budianu, M. Purica, D. Cristea, I. Cernica, R. Muller, V. Moagar Poladian, Solar Energy Materials & Solar Cells **87**, 423 (2005).
[6] D. Iencinella, E. Centurioni, R. Rizzoli, F. Zignani, Solar Energy Materials & Solar Cells **87**, 725 (2005).
[7] Philippe Lalanne, G Michael Morris, Nanotechnology **8**, 53 (1997).
[8] S-S. Tan, M. L. Reed, H. Han, R. Boudreau, J. Microelectromech. Syst. **5**, 66 (1996).
[9] A. J. Nijdam, E. Van Veenendaal, H. M. Cuppen, J. Van Suchtelen, M. L. Reed, J. G. E. Gardeniers, W. J. P. Van Enckevort, E. Vlieg, M. Elwenspoek, J. Appl. Phys. **89**, 4113 (2001).
[10] A. J. Nijdam, J. Van Suchtelen, M. L. Reed, W. J. P. Van Enckevort, E. Vlieg, M. Elwenspoek, J. Appl. Phys. **89**, 7 (2001).
[11] E. Vazsonyi, K. De Clercq, R. Einhaus, E. Van Kerschaver, Solar Energy Materials & Solar Cells **57**, 179 (1999).
[12] Drago Resnik, D. Vrtacnik, U. Aljancic, S. Amon, J. Micromech. Microeng. **13**, 26 (2003).
[13] Tabata O, Sensors and Actuators A **53**, 335 (1996).
[14] K. B. Sundaram, A. Vijayakumar, Microelectron Eng **77**, 230 (2005).
[15] Soonwoo Kwon, Jongheop Yi, Sewang Yoon, Joon Sung Lee, Donghwan Kim, Current Applied Physics **9**, 1310 (2009).
[16] J. T. L. Thong, W. K. Choi, C. W. Chong, Sensors and Actuators A **63**, 243 (1997).
[17] W. K. Choi, J. T. L. Thong, P. Luo, C. M. Tan, T. H. Chua, Y. Bai, Sensors and Actuators A **71**, 238 (1998).
[18] J. T. L. Thong, P Luo, W K Choi, S C Tan, J. Micromech. Microeng. **11**, 61 (2001).
[19] J. T. L. Thong, Y. Bai, P. Luo, W. K. Choi, Materials Science and Engineering B **72**, 177 (2000).
[20] Ou Weiying, Zhang Yao, Li Hailing, Zhao Lei, Zhou Chunlan, Diao Hongwei, Liu Min, Lu Weiming, Zhang Jun and Wang Wenjing, Journal of Semiconductors **31**, 10 (2010).
[21] A. V. Shah, J. Meier, E. Vallat-Sauvain, N. Wyrsch, U. Kroll, C. Droz, U. Graf, Solar Energy Materials & Solar Cells **78**, 469 (2003).

*Corresponding author: zamirlitho@gmail.com